Two-Terminal Molecular Memories from Solution-Deposited C_{60} Films in Vertical Silicon Nanogaps

David A. Corley,[†] Tao He,[†,‡] and James M. Tour[†,*]

[†]Departments of Chemistry, Computer Science, Mechanical Engineering and Materials Science, and the Smalley Institute for Nanoscale Science and Technology, Rice University, Houston, Texas 77005 and [‡]National Center for Nanoscience and Technology, Beijing 100190, China

ARTICLE

ABSTRACT We demonstrate here two-terminal, charge-based memory from C_{60} films inside vertical 7 nm silicon nanogap devices. This testbed structure eliminated the possibility of metal migration in the nanostructure because the two electrodes are made solely of silicon; hence, the often troublesome and confusing possibility of filamentary metal formation is obviated. Saturated solutions of C_{60} in toluene, mesitylene, and 1-methylnaphthalene were each used to deposit these films at elevated temperatures. Electrical *I*—*V* measurements reveal a high yield (67%) of devices demonstrating bipolar, switchable hysteresis from both the mesitylene- and 1-methylnaphthalene-deposited devices, while the toluene-grafted devices display no such behavior. Pulse-based memory measurements of switching devices indicate high ON/OFF ratios (maximum ~1500), good stability (>100 cycles without device degradation) for molecular devices, and low operating currents (~10^{-11} A) in room temperature testing.

KEYWORDS: C_{60} · fullerene · memory · two-terminal

Molecular electronics seeks to exploit the unique capability of molecular orbitals to modulate the transport of carriers in diminutive device structures. By combining bottom-up synthesis of molecular electrical elements with strategic molecular grafting techniques to larger silicon device structures, a practical fabrication methodology is sought. While molecules are thought to represent the pinnacle of density and power efficiency possible for electronic devices, issues with stability, speed, and reliability have remained challenges to the molecular electronics endeavor and have retarded their practicality in devices.[1] Despite these challenges, the desire to extend Moore's law into future decades has sustained scientific interest in the field.

In general, molecular electronics pursuits can be categorized into two general strategies: (a) those which pass current through the substrate whose transport properties are tuned by a surface molecular layer, and (b) those which pass current through molecular layers or individual molecules. Our recent surface grafting experiments[2,3] are good examples of the former, in which molecular monolayers are grafted onto silicon FET channel regions to adjust their threshold voltages. The latter through-molecule strategy has been employed in several memory devices with moderate successes from molecules assembled between metallic electrodes,[4−7] leading to two-terminal, molecular memory devices. While these are scientifically interesting, the stability and resilience of these systems limit their utility.

For molecular electronic studies, the use of metal electrodes offers advantages in ease of device fabrication and often allows for densely packed monolayers *via* thermodynamically controlled molecular self-assembly, as is the case with the prototypical thiol/gold system.[8] However, issues with metal migration and filament formation complicate the utility of metal electrodes, and this becomes exacerbated at the very short electrode gap distances needed to contact molecules.[9−11] This motivated the investigations here into fully nonmetallic electrodes to obviate the metal migration issues, which are common when several volts are applied across nanometer-sized electrode gaps.[12] Such migration issues mask and confuse molecular switching effects. Silicon's well-established manufacturing and characterization techniques make it an appealing design platform. However, despite its appeal, silicon lacks a molecular self-assembly protocol that is thermodynamically controlled; therefore, different strategies must be employed to apply the kinetically controlled molecular grafting through, for example, diazonium grafting and hydrosilylation.[13,14]

*Address correspondence to tour@rice.edu.

Received for review November 5, 2009 and accepted March 04, 2010.

Published online March 15, 2010.
10.1021/nn901566v

© 2010 American Chemical Society

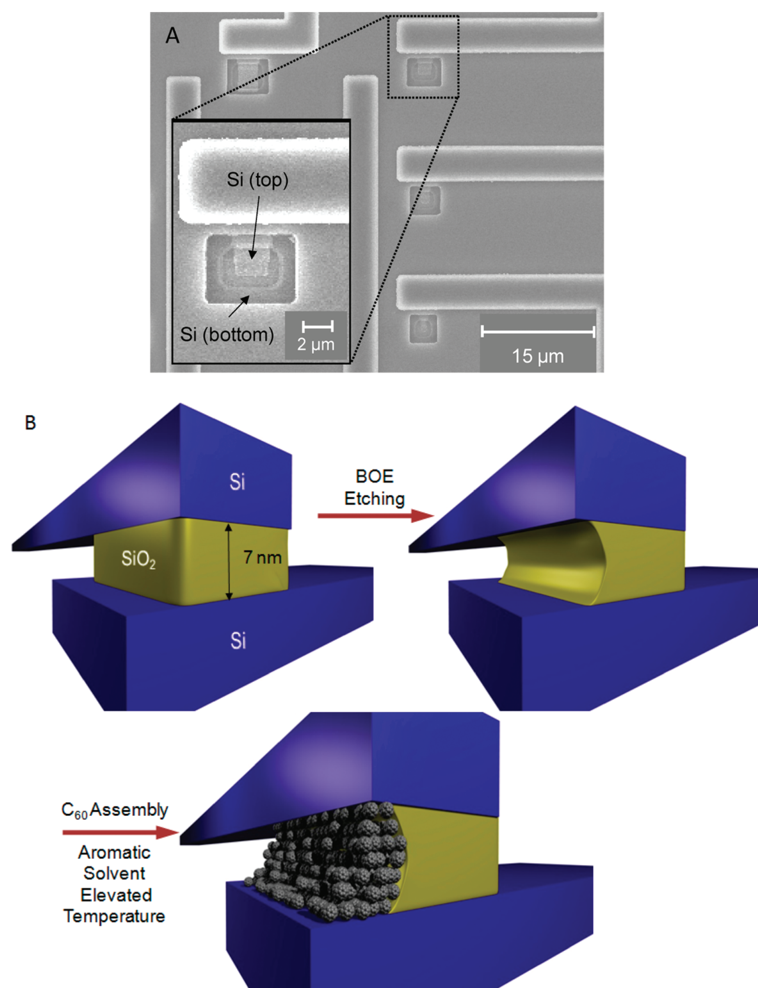

Figure 1. Silicon nanogap device structure. (A) SEM image of the nanogap devices from a top view that does not reveal the active region between the silicon electrodes. (B) Schematic of a pristine device, the device after etching, and the device after C_{60} deposition. The C_{60} film fills the gap formed in the 7 nm SiO_2 (yellow) layer between the top polysilicon electrode and the bottom silicon electrode (blue).

Our first attempt toward a metal-free, silicon-based design was the two-terminal molepore testbed, which utilized nanotubes as the top contact for molecules grafted onto a silicon substrate *via* diazonium salt grafting;[15] however, the nanotube/molecule interface added an additional component to the system that complicated interpretation of electrical results. We had also previously produced a metal-free, two-terminal, silicon-based nanogap vehicle for determining the electrical properties of embedded molecular species between vertical silicon electrodes that were nanometers apart; however, our initial application of the design used metallic nanoparticles to bridge molecular layers grafted onto each electrode and was therefore not truly metal-free.[16] In these one-dimensional nanogap devices,[16] shown in Figure 1, the gap structure consists of silicon top and bottom electrodes separated by a SiO_2 dielectric layer. After etching, this insulating layer is partially removed and the exposed silicon surfaces are hydrogen-passivated, which provides a surface that is reactive toward various molecular grafting techniques, including diazonium salt grafting[13] and hydrosilylation.[14] This allows for a Si/molecular film/Si sandwich structure in which the molecules may be added at a later stage in device fabrication, circumventing common problems with molecular stability under the high-temperature conditions necessary for solid-state device fabrication. Additionally, this late-stage grafting approach produces a structure in which the molecular film is not the structural support for the top electrode, nor is the quality of the top electrode limited by the quality of the film. This is the case for many metal/molecule/metal and metal/molecule/semiconductor sandwich structures, where the top electrode is deposited atop the molecular layer and film defects result in pinhole shorts and device failure.[12]

In selecting a species to graft into the nanogap in pursuit of a metal-free, molecular memory, a candidate was selected that had appropriate chemical and electrical stability, known chemistry for surface film formation and attachment, a potential to aggregate upon drying, and the potential for bias-driven switching behavior. Fullerenes have demonstrated interesting electrical behavior in solution and on surfaces[17−19] and are

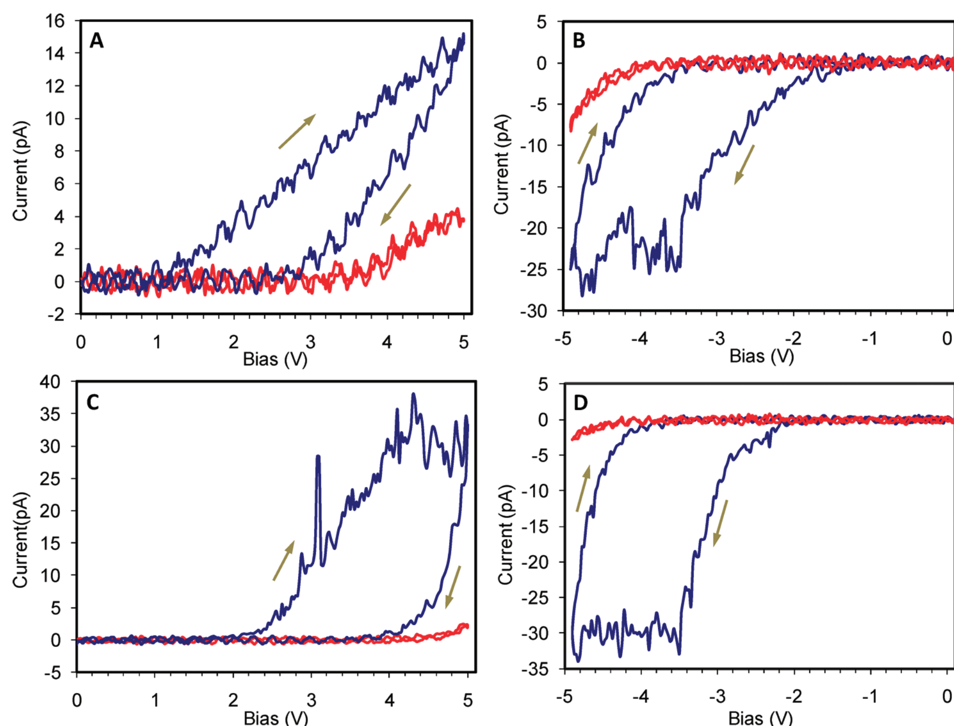

Figure 2. Typical *I*—*V* curves of switching silicon nanogap devices. (A,B) Mesitylene-deposited devices; (C,D) 1-methylnaphthalene-deposited devices. The red trace in each graph is the OFF-state of the device, prior to a sweep or pulse of the opposite bias. The blue trace in each graph is the ON-state for the device, after a sweep into the opposite bias direction, which follows a higher-conductivity path until the device is discharged at high bias and returns to a low-conductivity OFF-state.

good candidates for charge storage within organic polymers.[20] In addition to being one of the most studied molecules in the molecular electronics literature, C_{60} exhibits much of the thermal and chemical stability of its larger carbon nanostructured cousins, carbon nanotubes and graphene, but its well-defined integral structure results in an inherently more homogeneous material, lacking the polydispersity and inevitable structural defects introduced in the preparation and purification of larger dimensional carbon structures. When constructing electronic devices from C_{60} films, covalent attachment or physisorption of C_{60} directly to the electrode minimizes the distance and, therefore, poses some advantage over the use of tethers[21] by reducing the barrier for electron tunneling and charge injection from the substrate since there is no molecular alligator clip, which is often the predominant transport barrier in the device structure.[12] Here we report a facile method for solution-based deposition of C_{60} films directly onto hydrogen-passivated Si(111) surfaces and into hydrogen-passivated 7 nm silicon nanogap devices. Electrical measurements of the resulting nanogap devices reveal room temperature reliable (from a molecular electronics perspective) memory behavior with high ON/OFF ratio and good stability.

RESULTS

The *I*—*V* curves shown in Figure 2 demonstrate the bipolar switching behavior of successfully grafted 7 nm nanogap devices. C_{60}-grafted nanogap devices demonstrated operating currents in the 10^{-11} A range, as well as switchable hysteresis behavior, possessing ON/OFF ratios from 1 to 3 orders of magnitude. These devices could be reliably switched into a higher conductivity state by a pulse or a sweep of the opposite bias; the devices remained in this high-conductivity state until a sufficiently high bias was pulsed or swept, after which the device returned to a low-conductivity state. The device's ON-state was maintained as long as 12 h under vacuum, demonstrating relatively nonvolatile memory behavior within this timescale. However, the device's ON-state was quickly lost upon exposure to air, restricting device operation to the vacuum of the probe station. Of the measured devices, this switching behavior was observed for 67% of the mesitylene (6 out of 9) and 1-methylnaphthalene (6 out of 9) grafted samples, but not for any of the toluene-grafted samples.

The nanogap test chip includes control structures that are identical to the nanogap devices except that their oxide layer is protected by a layer of silicon nitride such that it cannot be etched; therefore, a nanogap cannot be formed.[16] Electrical measurements of such control structures aid in the differentiation of effects that are due to the molecular film from those that are inherent to the device structure itself. For these control structures, the observed current is in the noise level (10^{-13} A) with no hysteresis or switching behavior observed. Further control experiments were performed to

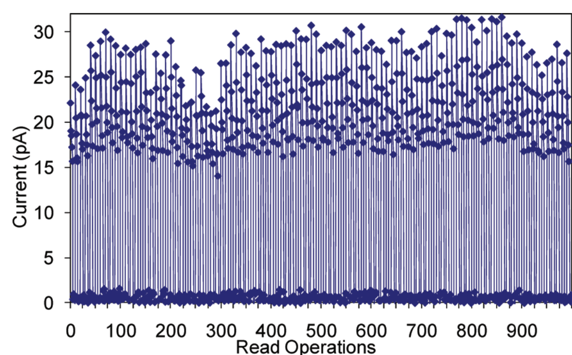

Figure 3. Measured device current during read operations from 100 device cycles in which one cycle corresponds to one write (−5 V, 20 s), five reads (2.5 V, 1 μs each), one erase (5 V, 20 s), and five reads (2.5 V, 1 μs each).

ensure that the observed behavior was not a product of the nanogap alone. $I-V$ measurements were performed on nanogap devices after only etching and drying and on devices that were exposed to the grafting conditions of solvent heating without C_{60} present. In both cases, it was clear that the C_{60} film provided device performance and stability, as many of these C_{60}-free devices experienced oxide breakdown at or below ±6 V, resulting in higher currents, unpredictable hystereses, and no switching behavior. In contrast, C_{60}-grafted samples could often be measured with bias sweeps up to ±7 V and long (60 s) pulses at ±6 V without device degradation. Devices from both sets of control experiments that did not experience oxide breakdown had currents in the noise level (10^{-13} A).

The effects of heating the grafted devices were studied to determine if thermal annealing could improve the yield of switching devices. C_{60}-grafted nanogap devices were annealed at 200 °C for 90 min, under argon, and then electrically characterized once again. The annealing process lowered the yield of switching devices for the mesitylene samples to 11% and the 1-methylnaphthalene samples to 44%. Annealing did nothing to activate switching in toluene samples. Similarly, cooling conditions were detrimental to the device structure. When devices were cooled to 100 K to determine if they could switch at cryogenic temperatures, the low temperatures physically altered the devices, all of which refused to switch either at low temperature or even after warming back to room temperature.

Memory measurements were performed using a pulse program consisting of a pulse in the negative bias (−5 V for 20 s) to set the device into an ON-state, followed by five consecutive read operations (2.5 V for 1 μs each), followed by an erase pulse (5 V for 20 s), and yet another five read operations (2.5 V for 1 μs each). Figure 3 demonstrates the stability of the device over 100 of these cycles without degradation, where the average observed ON/OFF ratio is about 15 using these read/write/erase conditions. For memory measurements of switching nanogap devices, in general, write times shorter than 5 s yielded inferior ON/OFF ratios,

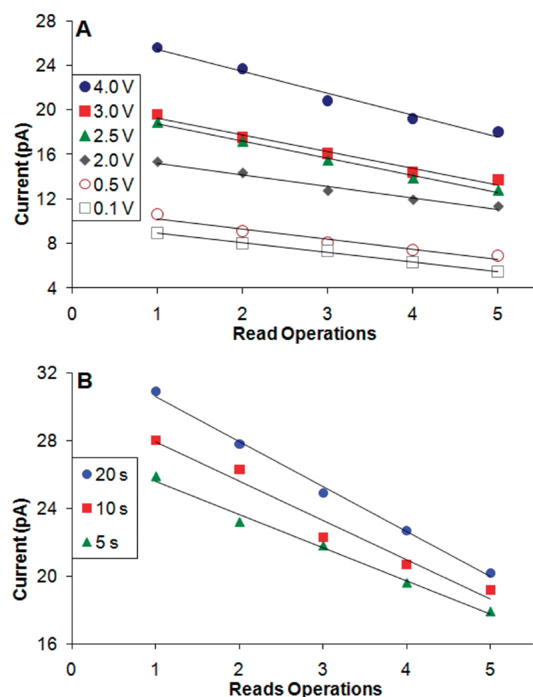

Figure 4. Diminishing ON-state current for five consecutive 1 μs read operations under varied read and write conditions. (A) After writing (−6 V for 5 s), the measured ON-current (pA) for the device across five consecutive read operations under different read bias (between 0.1 and 4.0 V). (B) After writing at −6 V for 5, 10, or 20 s, measured ON-current (pA) for the device across five consecutive (4 V) read operations.

demonstrating that C_{60}-grafted nanogap devices required several seconds of applied bias to turn completely ON; however, write times longer than 20 s provided no significant increase in ON/OFF ratio upon reading. The maximum ON-currents measured were small (tens of picoamperes) since they were restricted by the dimensions, interface barrier, and conductivity of the C_{60} thin film grafted within the nanogap device.

In order to improve the ON/OFF ratio for the switching nanogap devices, the effects of the read and write conditions on the device's ON-state were explored. As shown in Figure 3, repeated read operations performed after writing were slowly destructive to the ON-state; specifically, after writing the device to an ON-state, each successive read operation measured less ON-current than the previous operation until the device was rewritten and the ON-state was refreshed. The measured ON-currents of a nanogap memory device under various (Figure 4A) read biases and (Figure 4B) write times are presented. Each five-point data series represents the measured ON-current for five consecutive 1 μs read operations. For Figure 4, a constant write bias of −6 V was used because it represented the largest bias that could be reliably applied to the device for relatively long pulses (up to 60 s) without damaging the C_{60}-grafted devices. For each data series in Figure 4A, a −6 V write operation (not shown) was first performed for 5 s to turn the device ON, after which the declining ON-current was repeatedly measured using different read

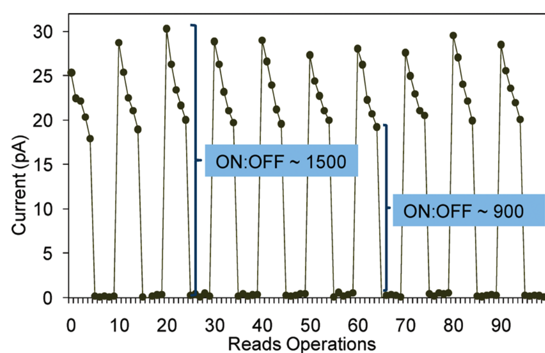

Figure 5. Read operations from 10 device cycles under improved conditions in which one cycle corresponds to one write (−6 V, 10 s), five reads (4 V, 1 μs each), one erase (6 V, 10 s), and five reads (4 V, 1 μs each).

biases. When a relatively high read bias was applied, the initial ON-current was higher than that observed for lower read biases, but the decline of the ON-current was steeper across repeated read operations. When a lower bias was employed for reading, the device's ON-current was initially lower, but the ON-current decline was not as steep during the repeated read operations. In Figure 4B, a −6 V write operation (not shown) was first performed for 5, 10, and 20 s to turn the devices ON, after which the ON-current was repeatedly measured using a constant read bias of 4 V. Here, when a longer write time was used, a higher initial ON-current was observed than for shorter write times, but the decline of the ON-current was steeper during the repeated read operations. When a shorter write time was used, a lower initial ON-current was observed, but the drop ON-current was not as sudden over repeated read operations. Therefore, at least at constant write bias and constant read time, there was a dependence of the decay of the ON-current during repeated read operations on both the read bias and the write time employed for measurement (see Supporting Information for a plot of the slopes of the lines in Figure 4 *vs* read bias and write time). From this, we selected values for read bias (4 V), write bias (−6 V), and write time (10 s) in order to improve the ON/OFF ratio of the nanogap devices, even for the fifth repeated read of a device's ON-state. Figure 5 shows 10 device cycles using these improved conditions, demonstrating a maximum ON/OFF ratio of about ∼1500 and a minimum ON/OFF ratio of ∼900 by the fifth read operation.

DISCUSSION

C_{60} film formation for most surfaces in the vapor phase is thought to proceed by an initial physisorption to the surface through dipole interactions. If these van der Waals forces between the surface and the C_{60} are sufficiently weak to allow movement, the initial absorbates will migrate to small defects, such as steps and troughs,[23−28] then serve as nucleation sites as van der Waals forces between the fullerenes themselves encourage film formation. While metals often show this weaker physisorption/migration phenomenon, the strength of the interaction on silicon depends on the presence of silicon dangling bonds. If present, these reactive dangling bonds strongly physisorb and anchor C_{60}, preventing migration, quickly followed by chemisorption, resulting in one or more covalent Si−C bonds to the surface.[28,29] If, however, these dangling silicon bonds are hydrogen-passivated, this interaction is weaker and migration is observed. Covalent attachment has also been observed from C_{60} in the vapor phase[30] and from solvent-cast films of C_{60} on hydrogen-passivated silicon substrates at elevated temperatures by hydrosilylation, resulting in cleavage of the Si−H bonds, formation of multiple Si−C bonds, and multiple reductions of the fullerene.[23] To date, most methods for C_{60} film formation involve vapor-phase, epitaxial growth of C_{60} films on silicon substrates within high-vacuum grafting chambers. In contrast, this work demonstrates the formation of thicker, multilayer C_{60} films on hydrogen-passivated silicon substrates during a heated, solvent-based grafting.

The electrical measurements indicated that the choice of deposition solvent played a role in the realization of switching behavior; mesitylene and 1-methylnaphthalene were capable of producing devices with switching behavior, while toluene was not. However, it is difficult to characterize the interfacial electronic states inside a 7 nm nanogap device structure to experimentally determine the source of the switching behavior with certainty. To facilitate further study, C_{60} films were simultaneously solvent-grafted onto hydrogen-passivated Si(111) surfaces to serve as macroscopic-scale analogues, allowing characterization that is not feasible within the miniscule confines of the nanogap device structures. The noncovalent interactions between C_{60} molecules within all of the solvent-grafted films are dominated by the same noncovalent intermolecular attractive forces that dominate all C_{60} solids (produced and defined by the nature of the C_{60} structure itself) and therefore offer no basis for the differences in the electrical behavior of the films. In contrast, XPS C1s analysis of each of the solvent-grafted C_{60} films can determine the degree of C_{60}−Si and/or C_{60}−C_{60} covalent bonding within each sample, allowing correlations to be made between the electrical properties and unique carbon bonding within the C_{60} films produced by each of the three grafting solvents.

The C_{60}-grafted Si(111) surfaces were first analyzed by ellipsometry. Although there was no visible film on the silicon surface, ellipsometric analysis indicated that a 4.2 nm film remained on the mesitylene- and 1-methylnaphthalene-grafted samples, while the toluene-grafted surface possessed a slightly thicker film at 4.8 nm. Though the film thicknesses (Table 1) were smaller than the 7 nm polysilicon−silicon gap of the devices, the 2 day assembly time should prove to be sufficient to fill the SiO_2-walled structure (Figure 1).

TABLE 1. Grafting Temperature, C_{60} Loading, and Film Thicknesses on Si(111)−H Substrates Based on Ellipsometry Measurements after Grafting for 2 Days

solvent	deposition temp (°C)	C_{60} concentration[22] (mg/mL)	film thickness (nm)
toluene	170	2.8	4.8
mesitylene	190	1.5	4.2
1-methylnaphthalene	260	33	4.2

XPS C1s analyses of the C_{60}-grafted Si(111) surfaces (Figure 6) indicated a strong carbon signal for all samples. The toluene-grafted sample provided the strongest C1s signal, in agreement with the ellipsometry data. To determine the relative contribution of the various components within the C1s signals, curve-fitting was performed on the C1s signal for each sample (Figure 6). Two clear features were observed that distinguish the toluene-grafted surface from the surfaces grafted using the other two solvents. First was the difference in the relative contribution of the C1s (282.5 eV) component for each sample, corresponding to an electron-rich Si−C species resulting from chemical bonding to the surface.[31] The smallest relative C1s (282.5 eV) contribution, and therefore the lowest degree of Si−C_{60} covalent bonding to the surface, was observed for the 1-methylnaphthalene-grafted sample (1%), followed by the mesitylene-grafted surface (7%), while the toluene-grafted surface possessed the largest signal (17%). Second, both a broadened C1s signal and a 12−14% larger relative C1s (286.0 eV) contribution were observed for the mesitylene- and 1-methylnaphthalene-grafted samples when compared to the corresponding signals of the toluene-grafted sample. While oxidation of the C_{60} film might produce a C1s (286.0 eV) signal, no correlation was observed between the relative intensity of the O1s (533.0 eV) signal and the C1s (286.0 eV) component for each sample. Rather, samples with larger O1s signals possessed a proportionally larger Si2p (103.5 eV) component, verifying SiO_2 as the primary source of the oxygen signal (see Supporting Information). However, covalent bonding between individual C_{60} molecules within surface-grafted C_{60} films has been observed to cause both C1s broadening and a C1s (286.0 eV) signal increase.[32] It could be that the higher temperature graftings in mesitylene and 1-methylnaphthalene activate $C_{60}-C_{60}$ [2 + 2] reactions[33] in the grafting solution, and the resulting C_{60} oligomers were sterically bulkier and electronically less reactive than C_{60} itself for covalent attachment to the Si surface. Hence, compared to the extensive covalent attachment of individual C_{60} molecules in the toluene-grafted C_{60} film, mesitylene and 1-methlynaphthalene grafting might both produce films consisting of a greater number of C_{60} oligomers physisorbed onto the surface.

To explain the switching behavior in the nanogap devices, a proposed mechanism must match the experimentally determined features of the device and switching behavior and properly address the observed differences in the electrical measurements and XPS analyses

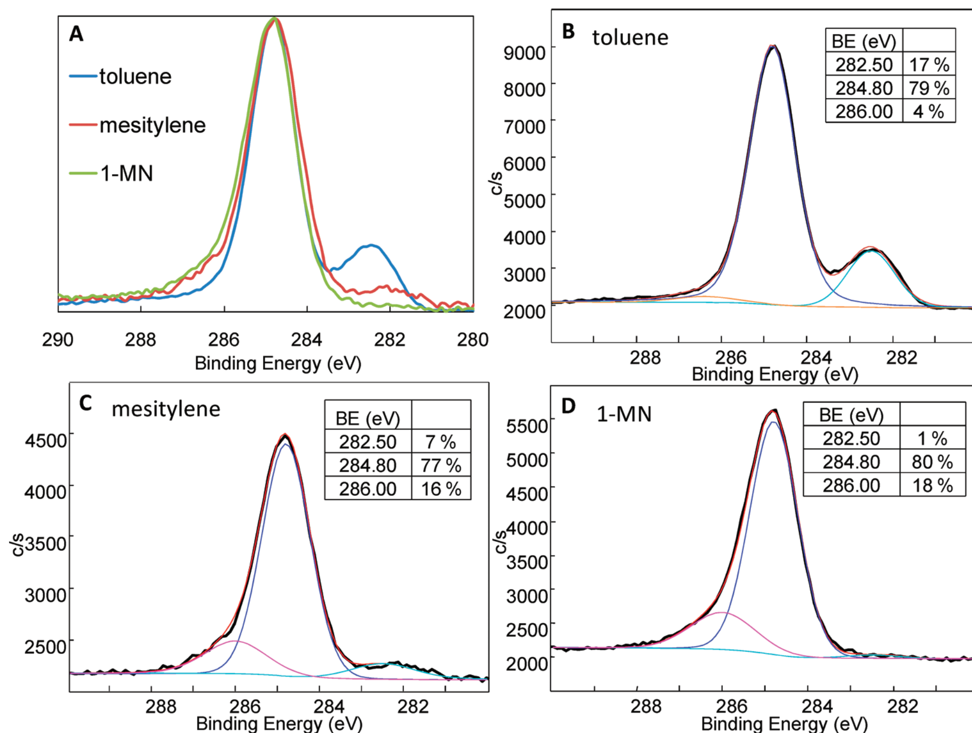

Figure 6. XPS analysis of solvent-grafted C_{60} films on Si(111) surfaces. (A) Superimposed view of XPS C1s signals for the C_{60} films on Si(111)−H for each solvent. Curve-fitting for C1s signals for (B) toluene, (C) mesitylene, and (D) 1-methylnaphthalene (1-MN) is included with relative contributions for each signal as an inset.

for the C_{60}-grafted samples produced by the three grafting solvents. While several physical phenomena could be suggested to explain the observed switching behavior, most are eliminated by the experimental details and results. First, the switching behavior is clearly not a result of the silicon platform itself. The bottom (n^+-Si) and top (poly-Si) electrodes of the device behave much like a conductor and, accordingly, cannot cause the resistance change observed during switching. The behavior cannot be attributed to metal filament formation as no metal is present in the active region, nor are the observed ON-currents sufficiently large to represent filamentary metal conduction. Additionally, since the two solvents that produced surfaces with the lowest (mesitylene) and highest (1-methylnaphthalene) relative oxygen concentrations (see O1s signals in Supporting Information) also produced switching nanogap devices, and since the toluene grafting produced a surface with medium oxygen concentration and no switching devices, it is unlikely that surface oxygen content played a role in either achieving or preventing switching behavior. Hence, processes sensitive to surface oxygen concentration, such as memory phenomena based on the movement of oxygen vacancies, are not likely candidates to explain the switching behavior. Finally, electrical measurements of Si control device structures that were identical in structure to the switching nanogap devices, except for the lack of either a nanogap opening and/or a grafted C_{60} film, failed to demonstrate switching behavior. This confirms that the switching behavior does indeed require a Si nanogap with a C_{60} film grafted inside.

Further, the measured ON-current of a switching nanogap device decreased over repeated read operations, even at low read biases, until the state was refreshed (Figure 4). A key feature associated with phase-change memory devices is the stability of their memory states beyond a decade,[1] even over many repeated read operations, without needing to refresh the device's state. Hence, a phase-change phenomenon is unlikely. State-destructive read operations are known within charge-based memory devices, including commercial one-time-read DRAM,[1] making a charging phenomenon a more likely candidate. A charge-trapping phenomenon is circumstantially supported by the complete loss of the ON-state of a device upon its exposure to air, as atmospheric components (O_2, H_2O, *etc.*) can quickly quench the trapped charge, turning the device OFF. Additionally, switching produced as the result of charge injection and trapping between the Si electrode and the C_{60} film (or Si/C_{60} interface) would be sensitive changes in the electrical contact between the film and electrode after the initial grafting is completed, as both the location of the charge traps and the electrical properties of the surface and film at the interface might be disturbed. Such a deleterious contact change is likely during the unequal expansion/contraction of the device structure and the C_{60} film (and/or thermal phase changes known to occur within C_{60} solids)[34] during heating and cooling treatments. Accordingly, the heating (200 °C) and cooling (100 K) experiments performed on C_{60}-grafted nanogap devices demonstrated that both treatments lowered the yield of switching devices considerably, providing further circumstantial evidence for a charging mechanism.

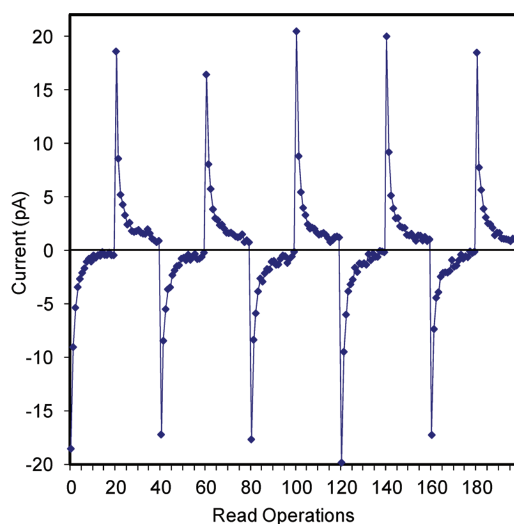

Figure 7. Read operations from 10 cycles demonstrating device behavior at 0 V read bias in which one cycle corresponds to one write (6 V for 20 s), 20 reads (0 V for 1 μs each), one write (−6 V for 20 s), and 20 reads (0 V for 1 μs each).

Additional evidence for a charging mechanism can be gleaned from further pulsed memory measurements. As seen in Figure 7, when read operations were performed without biasing the electrodes, the device was observed to charge equally well from either a positive (6 V, 20 s) or negative (−6 V, 20 s) pulse to subsequently demonstrate a negative or positive current, respectively, upon reading. Regardless of the write bias polarity used or the direction of the resulting current, the magnitude of the measured current asymptotically approaches 0 A over 20 consecutive unbiased 1 μs read operations. The presence of stored charge within the device after the ±6 V write pulse best explains the source of the electrical potential necessary to produce the currents measured in the absence of an externally applied read bias. With each unbiased read operation, the stored charge is depleted as it induces the current that is measured within the device, lowering the device's potential, thereby reducing the current measured for subsequent read operations. Additionally, the similarity in the magnitude of the measured current after a write pulse of either polarity, along the bipolar nature of the hysteresis observed in the $I-V$ curves of Figure 2, suggests that this charging may occur at either electrode with appropriate write bias polarity.

If a grafted C_{60} film were the only requirement for charge-based nanogap switching to occur, then we would expect switching behavior to be observed for

all samples grafted using solvents capable of producing a C_{60} film. However, switching behavior was not observed for toluene-grafted devices despite toluene forming a thicker C_{60} film on Si than the other solvents. Comparison of the XPS C1s analyses of each of the solvent-grafted C_{60} films demonstrated that the toluene-grafted sample possessed greater Si−C_{60} (and less C_{60}−C_{60}) covalent bonding than the samples grafted with the other two solvents.

We, therefore, hypothesize that the switching behavior observed in mesitylene- and 1-methylnaphthalene-grafted nanogap devices is caused by a resistance change due to a charge trapping phenomenon at the Si/C_{60} interface under an applied bias. When switching devices are placed under an applied bias, charge is trapped at the electrode/film interface, the resistance at the interface is reduced, and the conductivity of the system increases, yielding the ON-state. When an opposite bias is applied, these trapped charges are returned to the Si electrode, the resistivity of the interface increases, and the lower conductivity of the system is restored, yielding the OFF-state. For the toluene-grafted samples, however, the more extensive Si−C_{60} covalent bonding prevents charge from being effectively injected and/or trapped at the Si/C_{60} interface. This means that the toluene-grafted devices are locked in a permanent OFF-state because the Si−C_{60} covalent bonding either destroys the critical interfacial charge traps or creates an enhanced barrier for charge injection from the electrode surface such that the traps cannot be effectively charged within the compatible write bias range for the device. Accordingly, the 6% smaller relative C1s (282.5 eV) contribution observed for the 1-methylnaphthalene-grafted surface, representing less Si−C_{60} covalent bonding than the mesitylene-grafted surface, also explains the slightly larger hysteresis observed for the 1-methylnaphthalene-grafted nanogap devices during *I*−*V* analysis (Figure 2).

The choice of grafting solvent may play another role if solvent molecules were intercalated during film formation, which is known for aromatic solvents in C_{60} films.[35] These trapped solvent molecules would affect the resultant film structure and electrical properties by restricting electrical contact at both the Si/C_{60} and C_{60}/C_{60} interfaces, possibly even providing film defects that serve as charge traps. While they may contribute to the switching behavior observed in nanogap devices, the similarity in the C1s signals for the aromatic grafting solvents and C_{60} hinders discernment between the two,[36] leaving only circumstantial evidence to hint at the possibility of their existence. Under the vacuum of the electrical probe station, the relatively smaller, lighter toluene molecules would be more quickly liberated from the film than the relatively bulkier mesitylene and 1-methylnaphthalene molecules. If the presence of these solvent molecules were critical to switching, this would result in the attainment of switching devices from only mesitylene- and 1-methylnaphthalene-grafted devices, just as we have observed. This possibility is also supported by the fact that the 200 °C heat treatment induced a 33% greater drop in the yield of switching devices for the sample prepared with the smaller, lower-boiling mesitylene than for the sample produced using the larger, higher-boiling 1-methylnaphthalene. However, trapped solvent molecules offer no explanation for the differences in the C1s spectra of the different solvent-grafted surfaces discussed above and therefore cannot by themselves provide a full rationalization of switching behavior.

CONCLUSION

In conclusion, we have demonstrated two-terminal, charge-based memory from solvent-deposited, molecular films of C_{60} inside vertical 7 nm all-silicon nanogap devices. *I*−*V* measurements of nanogap devices demonstrate a high yield (67%) of bipolar, switching, memory devices from both the mesitylene and 1-methylnaphthalene grafting. Toluene-grafted devices showed no such switching behavior, and XPS C1s analysis revealed a greater degree of Si−C_{60} covalent bonding in toluene-grafted samples. Analysis of switching nanogap devices demonstrated high ON/OFF ratios (maximum ~1500), high stability for molecular systems (>100 cycles with no device degradation), and low operating currents (~10^{-11} A). By this approach of using only silicon electrodes at top and bottom, the often troublesome metal migration problem is obviated.

EXPERIMENTAL SECTION

All solvents were distilled and argon degassed prior to use. Toluene was distilled over CaH_2. 1-Methylnaphthalene was distilled over CaH_2 under reduced pressure. Mesitylene was distilled over molten sodium. All glassware was oven-dried or flame-dried prior to use. Buffered oxide etch (BOE, 6:1) was CMOS grade from J.T. Baker and was degassed at least 30 min with argon prior to use. C_{60} was purchased from MTD and used with no further purification.

Ellipsometry: C_{60} film thicknesses were measured with a single-wavelength (632.8-nm laser) LSE Stokes ellipsometer (Gaertner Scientific) with an incident angle of 70°. Ellipsometric characterizations were carried out before and immediately after film preparation. The surface thickness was modeled as a single adsorbing layer atop an infinitely thick substrate. The index of refraction (n_f) was set at 1.46. The reported thickness is the average value of five measurements from different locations of the sample's surface.

X-ray Photoelectron Spectroscopy (XPS): XPS data were collected at room temperature under ultrahigh vacuum (~10^{-9} Torr) using a PHI 5700 XPS/ESCA system (PHI Quantera SXM Scanning X-ray Microprobe) equipped with a monochromatic Al Kα light source (1486.6 eV) using a takeoff angle of 45°. The analytical spot size for all measurements was 0.10 mm × 0.10 mm. Measurements were performed with a pass energy of 6.5 eV. Data analysis was performed using the MultiPak Spectrum software, V7.01.

Solution-Based Deposition of C_{60} Films: Films were deposited from saturated[22] C_{60} solutions at different temperatures in three aromatic solvents: toluene, mesitylene, and 1-methylnaphthalene (Table 1). Si(111)−H shards were included with the nanogap device chips in each deposition run to allow for analysis by ellipsometry and XPS.

The devices and substrates were both etched in argon-degassed, BOE (6:1) for 2 min, then brought into a N_2 glovebox and heated to 120 °C for 5 min to ensure dryness. A screw-cap pressure tube was charged with C_{60} and freshly distilled solvent and then was mildly sonicated for 30 min as argon was bubbled through the solution. The pressure tube was then brought into the glovebox, and the devices and substrates were sealed inside. The pressure tube was then removed from the glovebox and then placed in an oil or sand bath, which was then covered with aluminum foil and heated at the deposition temperature for 2 days. After cooling, the samples were removed, thoroughly rinsed with toluene, and then dried under a stream of N_2.

Device Testing: The electrical characteristics of the devices were measured under vacuum ($<7 \times 10^{-4}$ Torr) using a semiconductor parameter analyzer (Agilent 4155C) and a probe station (Desert Cryogenics TTP4). The metal tips (ZN50R-25-BeCu, Desert Cryogenics) were probed directly onto the source/drain contacts using micromanipulators. Samples were placed under vacuum for at least 2 h before measurement. Measurements were made with an integration time of 640 μs. Read operations during pulsed memory experiments were performed at the lower limit (1 μs pulse width, 2 μs pulse period) of the device's pulse generator.

Acknowledgment. This work was funded by PrivaTran, LLC, through the SBIR program *via* the Army Research Office. We thank D.R. Wheeler and S.W. Howell of Sandia National Laboratory and H. Pang of Rice University for designing and fabricating the silicon nanogap structure.

Supporting Information Available: Slopes of trend lines, XPS spectra, and statistical analysis of the oxygen and silicon signals from the devices. This material is available free of charge *via* the Internet at http://pubs.acs.org.

REFERENCES AND NOTES

1. Galatsis, K.; Kang, W.; Botros, Y.; Yang, Y.; Ya-Hong, X.; Stoddart, J. F.; Kaner, R. B.; Cengiz, O.; Jianlin, L.; Mihri, O.; Chongwu, Z.; Ki Wook, K. Emerging Memory Devices. *IEEE Circuits Dev. Mag.* **2006**, *22*, 12–21.
2. He, T.; He, J.; Lu, M.; Chen, B.; Pang, H.; Reus, W. F.; Nolte, W. M.; Nackashi, D. P.; Franzon, P. D.; Tour, J. M. Controlled Modulation of Conductance in Silicon Devices by Molecular Monolayers. *J. Am. Chem. Soc.* **2006**, *128*, 14537–14541.
3. He, T.; Corley, D. A.; Lu, M.; Spigna, N. H. D.; He, J.; Nackashi, D. P.; Franzon, P. D.; Tour, J. M. Controllable Molecular Modulation of Conductivity in Silicon-Based Devices. *J. Am. Chem. Soc.* **2009**, *131*, 10023–10030.
4. Chen, J.; Reed, M. A.; Rawlett, A. M.; Tour, J. M. Large On−Off Ratios and Negative Differential Resistance in a Molecular Electronic Device. *Science* **1999**, *286*, 1550–1552.
5. Keane, Z. K.; Ciszek, J. W.; Tour, J. M.; Natelson, D. Three-Terminal Devices to Examine Single-Molecule Conductance Switching. *Nano Lett.* **2006**, *6*, 1518–1521.
6. Lörtscher, E.; Ciszek, J. W.; Tour, J. M.; Riel, H. Reversible and Controllable Switching of a Single-Molecule Junctions. *Small* **2006**, *2*, 973–977.
7. Reed, M. A.; Zhou, C.; Muller, C. J.; Burgin, T. P.; Tour, J. M. Conductance of a Molecular Junction. *Science* **1997**, *278*, 252–254.
8. Vuillaume, D. Molecular-Scale Electronics. *C. R. Phys.* **2008**, *9*, 78–94.
9. Stewart, D. R.; Ohlberg, D. A. A.; Beck, P. A.; Chen, Y.; Williams, R. S.; Jeppesen, J. O.; Nielsen, K. A.; Stoddart, J. F. Molecule-Independent Electrical Switching in Pt/Organic Monolayer/Ti Devices. *Nano Lett.* **2004**, *4*, 133–136.
10. Anaya, A.; Korotkov, A. L.; Bowman, M.; Waddel, J.; Davidovic, D. Nanometer-Scale Metallic Grains Connected with Atomic-Scale Conductors. *J. Appl. Phys.* **2003**, *93*, 3501–3508.
11. Lau, C. N.; Stewart, D. R.; Williams, R. S.; Bockrath, M. Direct Observation of Nanoscale Switching Centers in Metal/Molecule/Metal Structures. *Nano Lett.* **2004**, *4*, 569–572.
12. Tour, J. M. *Molecular Electronics: Commercial Insights, Chemistry, Devices, Architecture and Programming*; World Scientific Publishing Company: River Edge, NJ, 2003; pp 221−250.
13. Stewart, M. P.; Maya, F.; Kosynkin, D. V.; Dirk, S. M.; Stapleton, J. J.; McGuiness, C. L.; Allara, D. L.; Tour, J. M. Direct Covalent Grafting of Conjugated Molecules onto Si, GaAs, and Pd Surfaces from Aryldiazonium Salts. *J. Am. Chem. Soc.* **2004**, *126*, 370–378.
14. Buriak, J. M. Organometallic Chemistry on Silicon and Germanium Surfaces. *Chem. Rev.* **2002**, *102*, 1271–1308.
15. He, J.; Chen, B.; Flatt, A. K.; Stephenson, J. J.; Doyle, C. D.; Tour, J. M. Metal-Free Silicon-Molecule-Nanotube Testbed and Memory Device. *Nat. Mater.* **2006**, *5*, 63–68.
16. Howell, S. W.; Dirk, S. M.; Childs, K.; Pang, H.; Blain, M.; Simonson, R. J.; Tour, J. M.; Wheeler, D. R. Mass-Fabricated One-Dimensional Silicon Nanogaps for Hybrid Organic/Nanoparticle Arrays. *Nanotechnology* **2005**, *16*, 754–758.
17. Kadish, K. M.; Ruoff, R. S. *Fullerenes: Chemistry, Physics and Technology*; John Wiley & Sons Inc.: New York, 2000.
18. Porath, D.; Millo, O. Single Electron Tunneling and Level Spectroscopy of Isolated C_{60} Molecules. *J. Appl. Phys.* **1997**, *81*, 2241–2244.
19. Porath, D.; Levi, Y.; Tarabiah, M.; Millo, O. Tunneling Spectroscopy of Isolated C_{60} Molecules in the Presence of Charging Effects. *Phys. Rev. B* **1997**, *56*, 9829.
20. Mabrook, M. F.; Jombert, A. S.; Machin, S. E.; Pearson, C.; Kolb, D.; Coleman, K. S.; Zeze, D. A.; Petty, M. C. Memory Effects in MIS Structures Based on Silicon and Polymethylmethacrylate with Nanoparticle Charge-Storage Elements. *Mater. Sci. Eng., B* **2009**, *159*−*160*, 14–17.
21. Chen, B.; Lu, M.; Flatt, A. K.; Maya, F.; Tour, J. M. Chemical Reactions in Monolayer Aromatic Films on Silicon Surfaces. *Chem. Mater.* **2008**, *20*, 61–64.
22. Scrivens, W. A.; Tour, J. M. Potent Solvents for C_{60} and Their Utility for the Rapid Acquisition of ^{13}C NMR Data for Fullerenes. *J. Chem. Soc., Chem. Commun.* **1993**, 1207–1209.
23. Upward, M. D.; Moriarty, P.; Beton, P. H. Double Domain Ordering and Selective Removal of C_{60} on Ag/Si(111). *Phys. Rev. B* **1997**, *56*, R1704.
24. Sadowski, J. T.; Bakhtizin, R. Z.; Oreshkin, A. I.; Nishihara, T.; Al-Mahboob, A.; Fujikawa, Y.; Nakajima, K.; Sakurai, T. Epitaxial C_{60} Thin Films on Bi(0001). *Surf. Sci.* **2007**, *601*, L136–L139.
25. Loske, F.; Bechstein, R.; Schutte, J.; Ostendorf, F.; Reichling, M.; Kuhnle, A. Growth of Ordered C_{60} Islands on TiO_2(110). *Nanotechnology* **2009**, *20*, 065606.
26. Ueno, K.; Sasaki, K.; Nakahara, T.; Koma, A. Fabrication of C_{60} Nanostructures by Selective Growth on GaSe/MoS_2 and InSe/MoS_2 Heterostructure Substrates. *Appl. Surf. Sci.* **1998**, *130*−*132*, 670–675.
27. Hebard, A. F.; Zhou, O.; Zhong, Q.; Fleming, R. M.; Haddon, R. C. C_{60} Films on Surface-Treated Silicon: Recipes for Amorphous and Crystalline Growth. *Thin Solid Films* **1995**, *257*, 147–153.
28. Yao, X.; Workman, R. K.; Peterson, C. A.; Chen, D.; Sarid, D. The Bonding Nature of Individual C_{60} Molecules to Si(100) Surfaces. *Appl. Phys. A: Mater. Sci. Process.* **1998**, *66*, S107–S111.
29. Iizumi, K. i.; Saiki, K.; Koma, A. Investigation of the Interaction between a C_{60} Epitaxial Film and a Si(111)-7 × 7 Surface by Electron Energy Loss Spectroscopy. *Surf. Sci.* **2002**, *518*, 126–132.

ARTICLE

30. Feng, W.; Miller, B. Self-Assembly and Characterization of Fullerene Monolayers on Si(100) Surfaces. *Langmuir* **1999**, *15*, 3152–3156.
31. Santoni, A.; Frycek, R.; Castrucci, P.; Scarselli, M.; De Crescenzi, M. XPS and STM Study of SiC Synthesized by Acetylene and Disilane Reaction with the Si(100)2 × 1 Surface. *Surf. Sci.* **2005**, *582*, 125–136.
32. Onoe, J.; Nakao, A.; Takeuchi, K. XPS Study of a Photopolymerized C_{60} Film. *Phys. Rev. B* **1997**, *55*, 10051.
33. Rao, C. N. R.; Govindaraj, A.; Aiyer, H. N.; Seshadri, R. Polymerization and Pressure-Induced Amorphization of C_{60} and C_{70}. *J. Phys. Chem.* **1995**, *99*, 16814–16816.
34. Hamanaka, Y.; Norimoto, M.; Nakashima, S.; Hangyo, M. Raman Scattering of Solution-Grown and Vacuum-Deposited C_{60} Crystals. *Chem. Phys. Lett.* **1995**, *233*, 590–596.
35. Pozdnyakov, O.; Redkov, B.; Ginzburg, B.; Pozdnyakov, A. Trapping of Solvent by a C_{60} Fullerene Film. *Tech. Phys. Lett.* **1998**, *24*, 916–918.
36. Davis, D. J.; Kyriakou, G.; Lambert, R. M. Uptake of *n*-Hexane, 1-Butene, and Toluene by Au/Pt Bimetallic Surfaces: A Tool for Selective Sensing of Hydrocarbons under High-Vacuum Conditions. *J. Phys. Chem. B* **2006**, *110*, 11958–11961.